View metadata, citation and similar papers at core.ac.uk

brought to you by CORE

provided by Elsevier - Publisher Connector

Available online at www.sciencedirect.com

SciVerse ScienceDirect

Procedia Engineering 29 (2012) 2187 – 2193

Procedia Engineering

www.elsevier.com/locate/procedia

2012 International Workshop on Information and Electronics Engineering (IWIEE)

Design and Analysis of Multi-Winding Power Current Transformer for Power Transmission Lines Inspection Robot

Mingbo Yang[a]*, Zize Liang[a], Hanbo Qian[b], En Li[a], Guodong Yang[a]

[a]*State Key Laboratory of Intelligent Control and Management of Complex Systems, Institute of Automation, Chinese Academy of Sciences, Beijing 100190, P. R. China;*

[b]*The Center of Coordination&Support of SASTIND, Beijing 100081, P. R. China*

Abstract

Special current transformer (CT) is designed to induct power from the power transmission lines for an inspection robot. Equivalent circuit is used for calculating and modelling the parameters of the current transformer. Air gap analysis is given aiming at adapting dynamic range of bar current, and calculation of the effect of air gap is provided in detail. Ratio change of current transformer is introduced by which the secondary current could be adaptive to the bus current. Simulation results show that dynamic control of length of air gap and turns of the coils could make the current transformer be adaptive to the variable bus current and be more convenient for inducing power for the power transmission lines inspection robot.

© 2011 Published by Elsevier Ltd. Open access under CC BY-NC-ND license.

Key words: current transformer, induction charging, inspection robot

1. Introduction

In recent years, researchers have been working on designing one kind of mobile robots to partly or fully perform the inspection tasks of power transmission lines[1]~[3]. Most inspection robots are powered by Li battery packs. Due to the limitation of the Li battery capacity, the robot can not work continuously for a long time and requires periodical maintenance. So, continuous long period working ability of robot

* Corresponding author. Tel.: +86-015210146466.
E-mail address: jlsthsdqyx@sina.com.

1877-7058 © 2011 Published by Elsevier Ltd. Open access under CC BY-NC-ND license.
doi:10.1016/j.proeng.2012.01.285

becomes one of the vital difficulties before putting it into practical applications. To solve this problem, on-line power supply system is needed. Several available approaches have been tried on the robot such as laser power supply system, CT power supply system and solar power approach. Merits of laser power supply are the stable supplying of power and could be immune to the effect of bus current change, but due to the limited output power of laser and the low conversion efficiency of photocell, it is not fit for power the robot; solar power system has the same merits as those of laser's but it's performance is strongly effected by weather, and the price of this system is another shortcoming. Current transformer is used to induct power from power transmission lines by most of the researchers in this field. Merits of current transformer are of simple structure, low price, and easy to design, but this approach has its own shortcoming that is surging current in transmission lines. When the bus current is low, the device can not provide enough power for the robot, if the bus current becomes high, the CT would be saturated and heat consumption rises rapidly. Consequently, we must avoid such situations like that the device could not provide enough power for the equipment, or that the device could be destroyed by long time of deep saturation. In this paper, special current transformer will be designed to avoid or eliminate such situations for this application.

Similar work has been done and many means have been tried. In [4], a method to decrease the heat consumption of power supply by controlling the CT ratio is introduced. However, the author provides only two choices of turns of secondary winding, i.e., there are only two separated windings, so the secondary current could only alternate between two dynamic ranges of values. In [5], the author solves the problem of saturation and high heat consumption by introducing an air gap magnetic resistance to the draw-out coils and by matching parameters such as the configuration of the coil, the material of the magnetic core, turn numbers and air gap length. But the equivalent length of magnetic path is not provided by which we could control the permeability value of the current transformer by controlling the length of the air gap dynamically. In this paper, a multi-winding current transformer in introduced aiming at the problems mentioned above, and the experimental results which prove that the designed current transformer could have better performance in inducting power than conventional CT with no variable turns of coils and air gap.

2. Description of the induction unit

The inspection robot is designed for 500KV power transmission lines. In the design of this equipment, factors as insulation property, temperature characteristic and anti-interference ability of both software and hardware are considered, so in this paper, we are not going to talk about these details and we will focus on the design of the power induction equipment, the analysis and design of the current transformer.

Induction unit for power transmission lines inspection robot is equipped on the arm of the robot. Core of current transformer is divided into two semicircles and attached to one arm of the robot. When the robot negotiates with obstacles, the core opens up, moves upward and departs from the transmission line. During the normal inspection operations, the two semicircles will move downward, and close themselves to make a magnetic circuit for induction from the power transmission lines. The power induction unit is shown as Fig.1.

Normal bus bar current on power transmission lines varies between 5 ~ 1000 A, so the induction must be designed to work under this situation. Besides, abnormal situation such as short circuit with high impulse current should be considered to prevent the transformer from being destroyed.

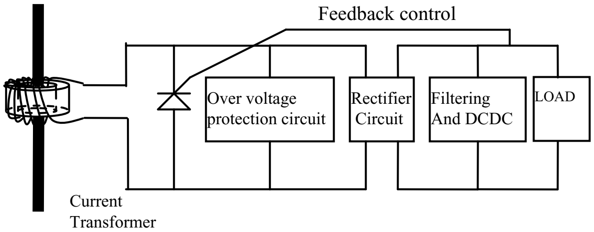

Fig.1 Schematic of induction circuit

3. Modeling and calculation of air gap

In general, air gaps can be very useful and desirable. Look at the B-H loop in Fig.2 the left one represents a hypothetical B-H curve for an un-gapped ferrite core. The right one represents the same core material with an air gap. We know that

$$B = \mu_0 \cdot \mu_r \cdot H \tag{1}$$

As Fig.2 shows, the maximum flux Bm density value at the onset of saturation is unchanged.

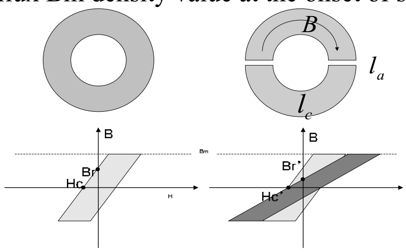

Fig.2 Characteristics of iron cores with air gap and magnetization curve

Main parameters of CT with air gap such as the permeability μ_e, the remanence B_r' and the maximum value of bus current I' are as follows,

$$\mu_e = 1 / \left(\frac{1}{\mu_c} + \frac{l_a}{\mu_a \cdot l_c}\right) = \mu_c / \left(1 + \frac{l_a}{l_c}\frac{\mu_c}{\mu_a}\right) \tag{2}$$

$$B_r' = B_r \cdot \frac{\mu_e}{\mu_c} = B_r / \left(1 + \frac{l_a}{l_c}\frac{\mu_c}{\mu_a}\right) = B_r / \left(1 + \frac{l_a}{l_c}\frac{B_r}{H_c}\frac{1}{\mu_a}\right) \tag{3}$$

$$I' = I \cdot \frac{\mu_c}{\mu_e} = I \cdot \left(1 + \frac{l_a}{l_c}\frac{\mu_c}{\mu_a}\right) \tag{4}$$

In order to take into account the air gaps in the theory of transformers, a modeling of the transformer joints is proposed as follows. The length of the equivalent air gap is assumed to be a function of the instantaneous value of the lamination flux showed as Fig.3. The corresponding effective permeability of the device has decreased and at the same time, its inductance in the linear region has also decreased. Since the equivalent air gap length is assumed to be constant, the air gap magnetic drop can neither give an account of local saturation, nor generate current harmonics [6]. Therefore, constant air gap could not justify the harmonic content of the magnetizing current especially under low saturation conditions [7].

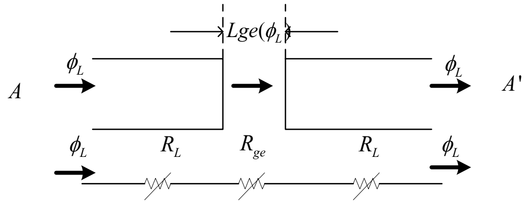

Fig.3 Schematic of nonlinear equivalent air gap

Where,

R_L Reluctance of iron core

R_{ge} Reluctance of air gap

All the reluctances are expressed as

$$R = \frac{1}{\mu}\frac{L}{S} \tag{5}$$

Where μ represents the permeability of magnetic dielectric, and L/S is the geometric characteristics of the corresponding magnetic flux path. Application of Ampere's law between A and A', using the equivalent nonlinear air gap circuit provides

$$\int_A^{A'} H dl = 2R_L\phi_L + R_{ge}\phi_L \tag{6}$$

$$R_{ge} = \frac{L_{ge}}{\mu_0 S} \tag{7}$$

Equation (6) and (7) provides the following relationship between L_{ge} and ϕ_L :

$$L_{ge} = (\int_A^{A'} Hdl - 2R_L\phi_L)\frac{\mu_0 S}{\phi_L} \tag{8}$$

Given the *B-H* characteristic from steel manufacturers for the range $0 \le B \le 1.9$ T, and using extrapolation for larger flux density [8], the established relationship between *H* and *B*:

$$H_{0<B<B_m} = c_1 B_L + c_2 sh(c_3 B_L)$$

$$H_{B>B_m} = \varepsilon\frac{|B_L| - J_s}{\mu_0} \tag{10}$$

Where ε = *abs(B)/B*, then,

$$L_{ge}|_{0<B<B_m} = (\int_A^{A'}(c_1 B_L + c_2 sh(c_3 B_L))dl - 2R_L\phi_L)\frac{\mu_0 S}{\phi_L} \tag{11}$$

$$L_{ge}|_{B>B_m} = (\int_A^{A'}(\varepsilon\frac{|B_L| - J_s}{\mu_0})dl - 2R_L\phi_L)\frac{\mu_0 S}{\phi_L} \tag{12}$$

Formula (11), (12) represents the relationship between equivalent length of the air gap, and the magnetic induction density under the situation of the given the B-H characteristic.

4. Power storage in air-gaped CT with multi-winding coils

As has been mentioned before, air gap is added in order to lower the magnetic permeability of the CT by which the CT could have higher value of *I'*, then, of course, the CT could have a good performance for the situation of high primary current instance. The air gap has a much higher reluctance than that of the magnetic material, so the reluctance of the air gap predominates. Flux is proportional to the magneto motive force divided by the reluctance. The flux density decreases for the same stimulus, and does the effective permeability. Inductance is a function of permeability so it decreases also. Also, the number of turns required to gain a given inductance has increased. With a small number of turns getting the desired inductance or transformation ratio for a transformer may be difficult. The induction of the current transformer could be represented using the following formula:

$$L = \frac{\mu_e N_2^2 S}{l_e + l_a} = \frac{\mu_e N_2^2 S}{l_{av}} \tag{13}$$

Power stored in CT can be calculated as follows:

$$W_1 = \frac{1}{2} L_1 I_{s1}^2 = \frac{1}{2} \frac{\mu_c N_1^2 S}{l_c} (\frac{I}{N_1})^2 = \frac{1}{2} \frac{\mu_c S}{l_c} I^2 \tag{14}$$

$$W_2 = \frac{1}{2} L_2 I_{s2}^2 = \frac{1}{2} \frac{\mu_e N_2^2 S}{l_c + l_a} (\frac{I'}{N_2})^2 = \frac{1}{2} \frac{\mu_e S}{l_c + l_a} I'^2 \tag{15}$$

Formula (2), (4), (14) and (15) can be combined to give an expression for the comparison of energy stored in both CT, so

$$\eta = \frac{W_2}{W_1} = \frac{l_c}{l_c + l_a} \frac{\mu_e}{\mu_c} (\frac{I'}{I})^2 = \frac{\mu_a \cdot l_c + \mu_e \cdot l_a}{\mu_a \cdot l_c + \mu_a \cdot l_a} \tag{16}$$

As $\mu_a << \mu_e$, so $\mu_a \cdot l_c$ can be eliminated, then

$$\eta = \frac{W_2}{W_1} = \frac{\mu_a \cdot l_c + \mu_e \cdot l_a}{\mu_a \cdot l_c + \mu_a \cdot l_a} \approx \frac{\mu_e}{\mu_a} \tag{17}$$

Here, η represents the ability of power storage between CT with air gap and CT without air gap. N_1, N_2 are reduced as the functions showed, so multi-winding can not improve the ability of the CT to output more power by induction.

5. Experiments and simulation results

The equivalent circuit of a current transformer with a mixed load is shown in Fig.4

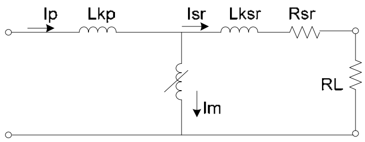

Fig.4 Equivalent Circuit Schematic

Parameters are set according to Fig.4 so that some characteristics of the CT could be expressed by changing the value of the equivalent circuit. Simulation results are showed in the following pictures. Fig.5 and Fig.6 displays only 4 different turns of the multi-winding CT so we can check out their curves clearly. Fig.5 displays the magnetic induction of the 4 situation. Fig.6 shows the secondary current of the multi-winding current transformer. The other 4 curves are output current of secondary winding with transformation ratio respectively as 1:10, 1:100, 1:200, 1:800, and turns of primary winding is 1.

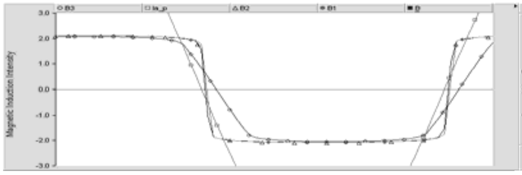

Fig.5 *B*-curves of the multi-winding current transformer

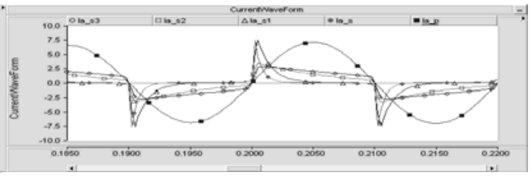

Fig.6 Secondary output current of the multi-winding current transformer

In Fig.5, as the secondary turns increased, B curves of the device becomes smoother and the saturation degree is reduced, which means that the using of multi-winding CT could improve the maximum saturation current of the device. Fig.6 shows the magnetic induction density of the CT, and approves the change of the saturation degree of the device according to the secondary turns of coils.

Fig.7 shows the B-H loop of the device which is based on the Jiles–Atherton (JA) phenomenological model of core in PSCAD. Here, the model is used to show the trends of the CT characteristics.

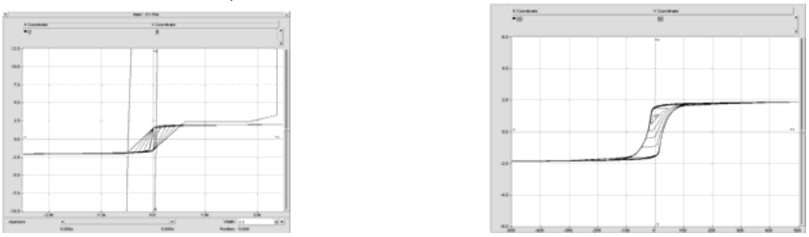

(A) (B)

Fig.7 B-H loop of CT with different turns of windings

Figure A and B shows two cases of the multi-winding CT. Figure A's ratio is 1:10, and Figure B's is 1:700. *B-H* loops are different. In figure A, when AC current becomes stable, the *B-H* curve moves out of the figure and becomes very sharp, the device is in deep saturation. In figure B, the situation is not the same as A. The CT *B-H* curve goes into the state of convergence, and transforms from saturation state to un-saturation state periodically. This shows a trend of changes of turns and length of air gap. So, device works with this principle could avoid saturated state in great degree and shows good performance in inducting power for inspection robot.

6. Conclusion

Special current transformer for powering the transmission lines inspection robot is introduced. Detailed analysis of this multi-winding design and the function of air gap are given. Simulation of this current transformer is provided which shows that the multi-winding CT with variable length of air gap could have good performance on *B-H* characteristics and could have better performance in inducting power for inspection robot from power transmission lines than conventional ones.

References

[1] S.Peungsungwa1, B. Pungsiri, K. Chamnongthai and M. Okuda. Autonomous robot for a powertransmission line. The 2001 IEEE International Symposium on. 2001 , Page(s): 121 - 124 vol. 2

[2]Jun Sawada, Kazuyuki Kusumoto, Yasuhisa Maikawa, Tadashi Munakata, Yoshinobu Ishikawa. A Mobile Robot For Inspection Of Power Transmission Lines. IEEE Transactions on Power Delivery, Vol. 6, No.1, January 1991.

[3]Hector Beltran, San Segundo, Vicente Fuster, Lourdes Perez, Pedro Mayorga. Automated Inspection of Electric Transmission Lines:The power supply system. 1-4244-0136-4/06. IEEE, 2006

[4]Qi Dong. A Kind of Power Supply of Optic-electric Current Transformer for Accommodating Wide Bus Dynamic Current. Proceedings of the CSEE. Vol.26 No.19 Oct. 2006

[5]Li Xianzhi, Du Lin, Chen Weigen, Wang Youyuan, Sun Caixin, Li Jing. A Novel Scheme of Draw-out Power Supply Utilized in Transmission Line State Monitoring. Automatino of Electric Power System. No.10 Jan. 2008

[6] M. Elleuch and M. Poloujadoff, “Three phase, three limb transformer model for switching transient calculations. Part I: Parameter definition and identification,” Acta Tech. CSAV, no. 1, pp. 100–117, 1988.

[7] M. Elleuch and M. Poloujadoff, “Contribution to the modeling of the transformer joints using a new concept of equivalent variable air-gap length,” Acta Tech. CSAV, no. 42, pp. 245–262, 1997.

[8] Mohammed Elleuch, Michel Poloujadoff. New Transformer Model Including Joint Air Gaps and Lamination Anisotropy. IEEE TRANSACTIONS ON MAGNETICS, VOL. 34, NO. 5, SEPTEMBER 1998